

Lightweight electrowetting display on ultra-thin glass substrate

Han You
Andrew J. Steckl

Abstract — Mobile display devices that use ultra-thin ($\leq 100\ \mu\text{m}$) glass substrates offer a combination of attractive characteristics: lightweight, high quality device fabrication process, thermal and dimensional stability, and mechanical flexibility. Electrowetting (EW) devices fabricated on ultra-thin glass are demonstrated in this paper. Water contact angle, which is the most critical parameter of EW devices, changes from $\sim 165^\circ$ to 80° when a 20 V direct current (or alternating current) voltage is applied. EW devices on ultra-thin glass show negligible hysteresis ($\sim 2^\circ$) and fast switching time of $\sim 10\ \text{ms}$. EW device operation is maintained when the glass substrate is mechanically flexed. These results indicate the promise of narrow profile EW devices on ultra-thin glass substrate for mobile and other devices, including video rate flexible electronic paper.

Keywords — *electrowetting, ultra-thin glass, contact angle, flexible display.*

DOI # 10.1002/jsid.169

1 Introduction

The development of new applications for electronic displays requires devices that are increasingly thinner, lighter, and flexible.^{1–5} This is particularly true in the field of mobile devices, such as smartphones, ultrabooks, and e-reader devices, where there is a major interest to produce lightweight and thin devices, with form factors that can be non-planar, or even can be folded for packing and unfolded for use. Ultra-thin displays are expected to play an increasing role in many applications, ranging from newspaper-like displays,^{6,7} radio-frequency identification tags,⁸ displays worn on the body, and toys and packaging.^{9,10} For portable applications, users need devices that work well in bright lighting conditions and have a long battery lifetime, requirements which point to the use of reflective display technologies.¹¹ Because of its operational characteristics, such as low power consumption, bistability, high reflectivity, and high switching speed,¹² electrowetting (EW) technology is a very promising candidate for electronic paper (e-paper) applications. The EW light valve is controlled by the motion of two immiscible liquids (one polar, the other nonpolar and one clear, the other colored) under the influence of an electric field.^{13,14} The EW light valve approach is quite versatile, leading to many important applications. Currently, the major application of EW technology is in the field of flat panel display.¹⁵ EW displays with multiple colors have been achieved without the use of color filters by using a vertical stack structure on a fixed glass substrate.¹⁶ Recently, EW operation on paper and different flexible substrate was shown to have switching

speeds that are promising for video display applications.^{17–19} Because of these attractive properties, EW displays continue to have great potential among emerging portable e-paper applications.

To achieve lighter and thinner portable displays for e-paper devices, most manufacturers generally consider replacing conventional glass substrates with lightweight polymer substrates. However, polymer substrates are known to suffer from reliability issues (such as gas permeation and material stability) and thermal and dimensional instability.²⁰ These instabilities lead to deformation and alignment issues while fabricating and assembling devices. For the EW-based displays, an ideal substrate would be able to withstand fabrication temperatures of $\sim 200^\circ\text{C}$ (not generally possible with plastic substrates) and not suffer from dimensional distortion during device fabrication.

Ultra-thin glass substrates with a thickness $100\ \mu\text{m}$ have been developed and utilized in the fabrication of organic thin-film transistor and liquid-crystal displays.^{21–23} In this paper, we report on the fabrication and operation of EW devices using Corning® Willow™ Glass (Corning Incorporated, Corning, NY, USA) which is a $100\ \mu\text{m}$ ultra-thin glass substrate. Individual EW devices with Willow Glass substrate have shown very promising EW properties, including large contact angle (CA) change ($\sim 80^\circ$), negligible hysteresis ($\sim 2^\circ$), and fast switching times of $\sim 10\ \text{ms}$, which is comparable with performance on conventional glass substrates. An EW array prototype fabricated on Willow Glass substrate can be switched reversibly by applying a low voltage. These results indicate the promise of Willow Glass as substrate for video rate flexible EW-based portable displays.

Received 02/27/13; accepted 06/19/13.

The authors are with Nanoelectronics Laboratory, Department of Electrical Engineering and Computing System, University of Cincinnati, Cincinnati, Ohio 45221–0030, USA; e-mail: a.steckl@uc.edu.

© Copyright 2013 Society for Information Display 1071-0922/13/2105-0169\$1.00.

2 Experimental details

A diagram of the EW structure on a 100- μm ultra-thin glass substrate is shown in Fig. 1. The EW structure is built on a glass bottom substrate and consists of a ground electrode, a dielectric layer, and a fluoropolymer layer. A top plate consisting of glass and electrode is used to complete the structure for array fabrication. A stable and thin substrate is a pronounced advantage to achieve good layer-to-layer alignment for a full color stack structure. Furthermore, by utilizing a glass substrate that is 5–10 times thinner for each of the three colors in the stack, one reduces not only the overall thickness and weight of the array but also optical distortions (such as parallax). Glass is not susceptible to localized dimensional distortion at the relatively low temperatures used during the process and is unaffected by the process chemicals utilized, unlike polymer films. These positive characteristics enable efficient overall device processing.

Indium tin oxide (ITO) electrodes were sputtered in argon at 3.5 mTorr with 150 W direct current (DC) power for 20 min. Next, a 100-nm Al_2O_3 layer was deposited via atomic layer deposition at 250°C (Cambridge Nanotech Savannah 100 ALD system, Cambridge Nanotech Inc., Waltham, MA, USA). The fluoropolymer (CYTOP CTL-809M, Ashahi Glass Co., Ltd. Tokyo, Japan) layer was then spin-coated to achieve a hydrophobic surface, forming a ~40-nm film. Details of the device fabrication process have been previously described.¹⁸ Atomic force microscopy (AFM) (Veeco Dimension AFM, Veeco, Plainview, NY, USA) was used to characterize the surface morphology. EW tests were performed in a mixture of

electrically insulating silicone oils (80 wt% Dow Corning OS-20, 10 wt% OS-10, and 10 wt% OS-30, Dow Corning Corporation, Midland, MI, USA). A clear acrylic box was used to contain the immersed substrate and fluids. A ~0.2 or 2- μL conducting fluid droplet was placed on the substrate and viewed through the transparent acrylic sidewalls for contact angle and switching speed testing, respectively. To provide electrical bias to the water solution, a wire probe was inserted into the polar droplet. The other end of this probe was connected to the voltage supply. An FTA 1000B contact angle measurement system (First Ten Angstroms Inc., Portsmouth, VA, USA) was used to record the contact angle data and the interface tension by the pendant drop method. DC and alternating current (AC) voltages up to 20 V were applied. The experiments were repeated at three or more locations with fresh samples for each test.

For the circular device, the hydrophilic grid was formed using a negative photoresist (SU-8 2010, MicroChem Corp. Newton, MA, USA). SU-8 was spin-coated forming a ~10- μm film, which was then patterned to form circular openings with 1.4 mm in diameter. Next, a hydrophobic grid of polyimide-based tape (Dupont™ Kapton® McMaster Carr, Aurora, OH, USA) was used to contain the water droplet. To operate the EW device, typically, a ~40 μL droplet of Deionized (DI) water is placed on the hydrophobic surface. Then, ~40 nL of dodecane oil (Acros purchased from Thermo Fisher Scientific Inc., NJ, USA) with a nonpolar red dye (Keystone Aniline Corp Chicago, IL, USA) is injected using a nano-injector system (Stoelting Co., Wood Dale, IL, USA). The oil injection process was

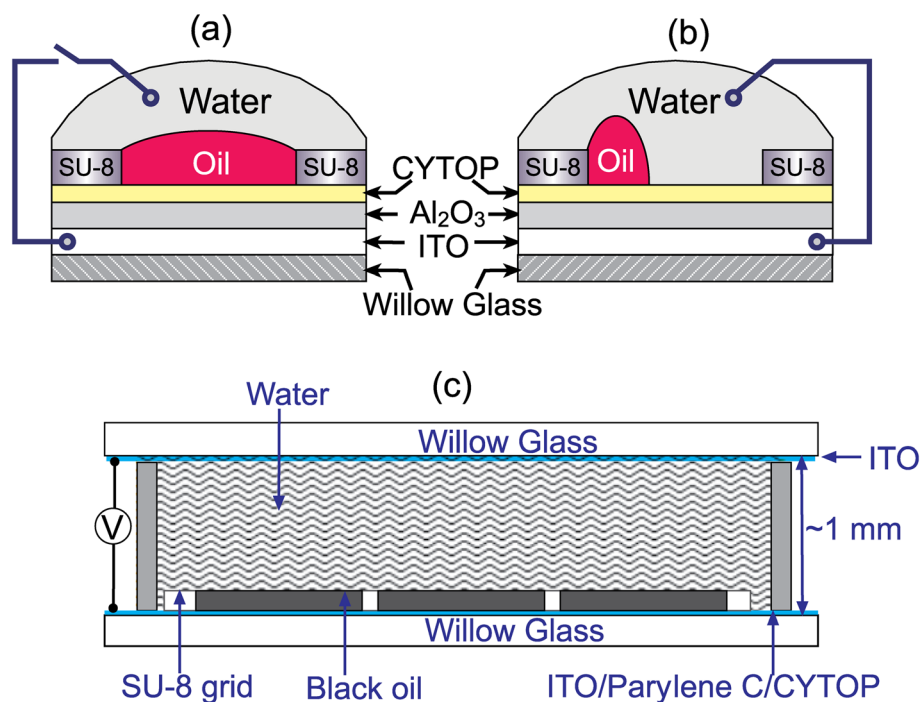


FIGURE 1 — Schematic diagrams illustrating the electrowetting (EW) operation on the Corning® Willow™ Glass substrate: (a) EW pixel without bias; (b) EW pixel with bias; and (c) completed EW array using Willow Glass as both the substrate and the top sealing plate.

monitored by a color charge-coupled device camera system (Diagnostic Instrument Inc., Sterling Height, MI, USA) in top view and charge-coupled device color video camera system (Sony USA, New York City, NY, USA) with TV zoom lens (Navitron, D. O. Industries Inc., East Rochester, NY, USA) for the side view.

3 Results and discussion

The morphology of the top surface will clearly influence the EW characteristics. Figure 2 contains AFM images of Willow Glass at different stages during the structure fabrication process. The inserts show the root mean square (RMS) roughness values of the corresponding surface at each step. The as-received glass (Fig. 2a) exhibits a very smooth surface morphology with an RMS value of 0.38 nm. After electrode (200-nm ITO) and insulator (100-nm Al₂O₃) deposition, the surface roughness (Ra) exhibits a slight increase. Interestingly,

after CYTOP spin-coating, the Ra is 0.38 nm, equal to the initial value. Apparently, the CYTOP acts as a planarizing layer.

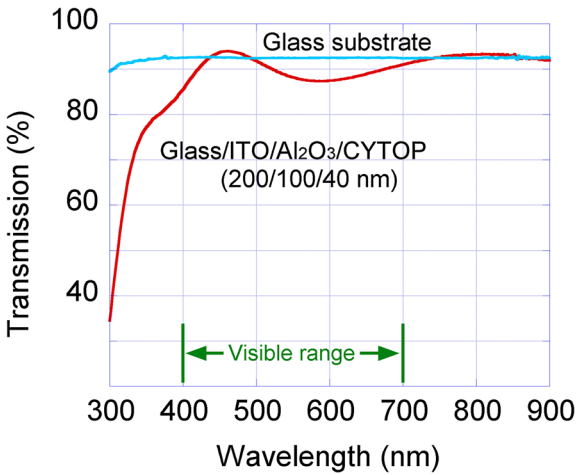


FIGURE 3 — Optical transmission of the electrowetting stack on Corning® Willow™ Glass.

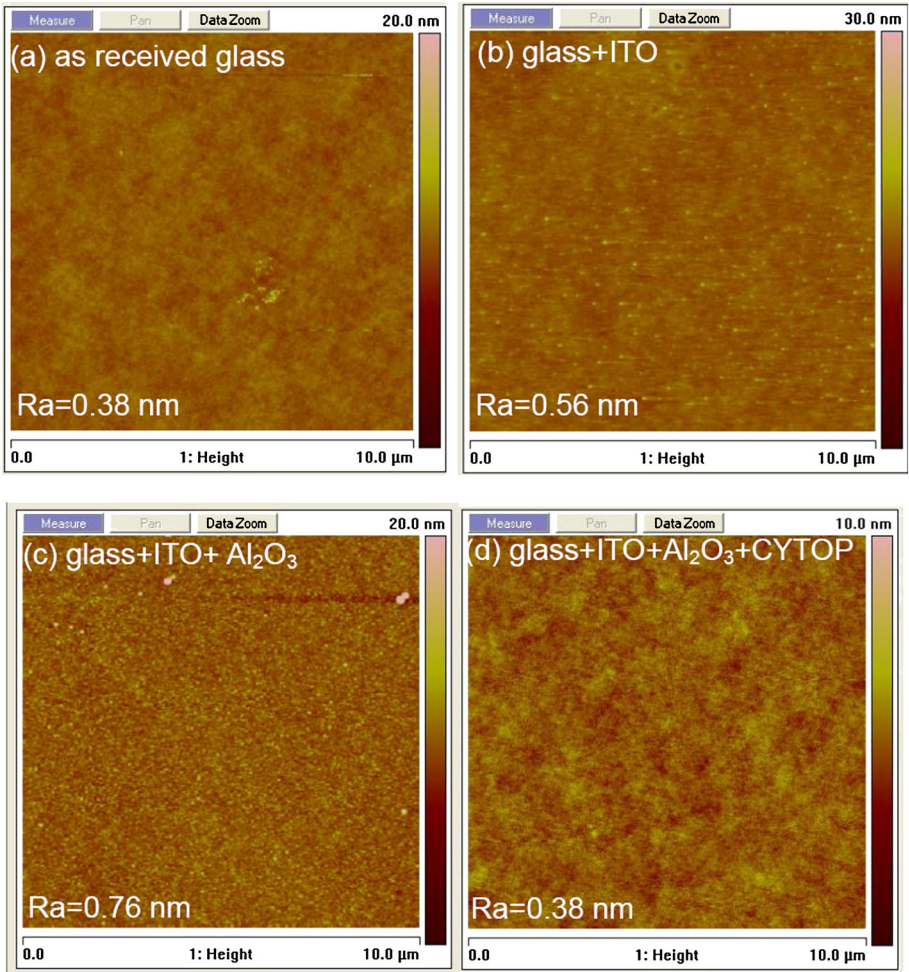


FIGURE 2 — Atomic force microscopy images and corresponding surface roughness of the EW structure at different stages in the device fabrication process (a) as received Corning® Willow™ Glass substrates; (b) glass with indium tin oxide (ITO) (200 nm) electrode layer; (c) glass with ITO and alumina (100 nm) insulating layer; (d) glass with ITO, alumina, and CYTOP (40 nm) fluoropolymer layer. Note: same in plane scale, different vertical magnifications scale.

Figure 3 shows the optical transmission of the EW structure after fabrication on Willow Glass. This structure has very high transmission in the visible (400–700 nm) range. The drop-off in the 300–400 nm region is ascribed to the absorption of the ITO electrode. The Willow Glass substrate itself exhibits uniformly high transmission (>90%) over the entire (300–900 nm) wavelength range.

The EW effect was first evaluated by measuring the CA of conductive aqueous fluid (0.05 M KCl) droplets immersed in a mixture of silicone oils (OS-20:OS-10:OS-30 = 8:1:1) as a function of the applied DC and AC voltages. In general, the maximum voltage used in this EW device is 20 V in order to prevent dielectric breakdown, which typically occurred at ~25–30 V for these devices. As shown in Fig. 4a, the initial CAs of 0.2 μ L KCl droplet in oil on the CYTOP surface is ~164°, decreasing to ~80° as the DC voltage increases to ± 20 V. Reversing the direction of the voltage sweep, the CA of the droplet recovered to the initial value (~164°). However, a relatively large hysteresis was observed at intermediate values of negative (and to a lesser degree positive) bias. For example, a hysteresis of 12° was present at –8 V. For AC bias, a 1-kHz square-wave signal was applied to the KCl droplet. The CA versus AC voltage

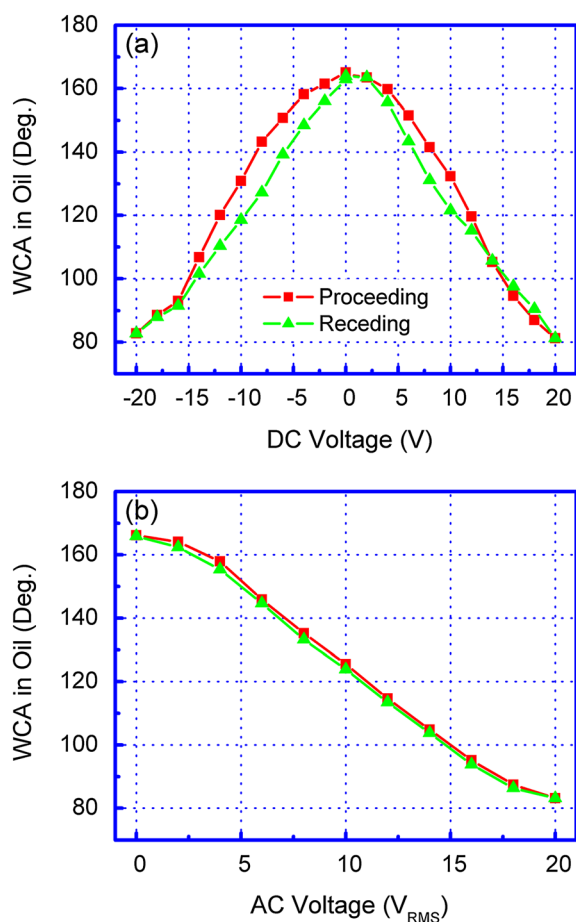


FIGURE 4 — Contact angle of 0.2 μ L water (0.05 M KCl) droplet in silicone oil as a function of applied bias (a) DC voltage and (b) 1 kHz square wave AC voltage (root mean square).

(RMS values) is shown in Fig. 4b. A change in CA of 82° is obtained between zero bias and 20 V RMS, which is roughly the same as for the DC voltage case. Most importantly, the hysteresis was greatly reduced in the AC bias mode, with a maximum value of <2°. This is the result of reduced charge injection into the fluoropolymer caused by a time lag between the applied electric field and the motion of charges in the structure.²⁴

Circular devices were also fabricated on the 100- μ m Willow Glass substrate to test the EW pixel operation through oil coverage change with applied voltage. The EW device operation principle without and with the applied voltage is illustrated in Figs 1a and 1b, respectively. The basic two-fluid EW device utilizes a conducting (water/electrolyte) and an insulating (oil) liquid. Fluid motion in the device is governed by the electric field applied to the water through the competitive EW effect. Oil coverage as a function of voltage for the two-fluid EW devices on flexible glass substrate is shown in Fig. 5. The EW device at zero bias has 100% oil coverage. The area covered by oil decreases to ~30% of the total device area as the bias is gradually increased to –20 V. When the bias is then decreased to 0 V, the displaced oil returns to full device area coverage. This process is repeatable many times as the applied voltage is varied.

The speed with which the water droplet changes CA under the influence of applied voltage determines the speed of the associated EW devices. The step response of the EW device on 100 μ m Willow Glass substrate was measured to determine the switching time. A 12 V voltage step of 500 ms duration with fast (2 ns) rise and fall times was applied to the 2 μ L KCl (0.05 M) water droplet in silicone oil ambient. The transient process was captured by using a high-speed camera (TSHRMS, Fastec Imaging Corp., San Diego, CA, USA) at 1000 fps. The contact length between the water droplet and CYTOP surface is monitored as it varies under the influence of voltage. The overall results of the contact length versus time during the application of voltage are shown in Fig. 6a. The magnified switch-on and switch-off segments of the process are shown in Fig. 6b. Fig. 7 shows the droplet wetting (Fig. 7a)

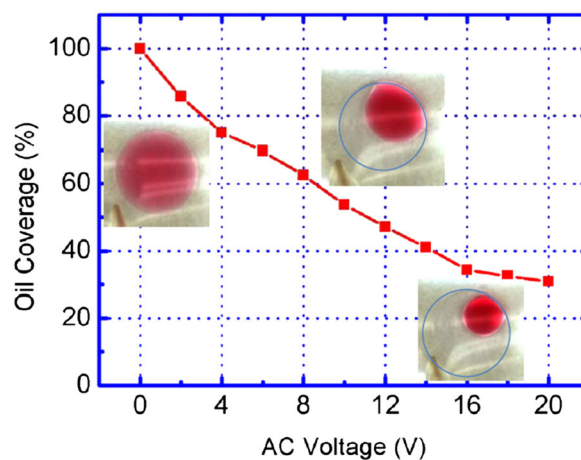


FIGURE 5 — Operation of a circular electrowetting pixel (1.4 mm diameter) covered by colored oil (60 nL of dodecane) as a function of 1 kHz square wave AC voltage (root mean square); insets show photographs of an electrowetting pixel at several voltage levels.

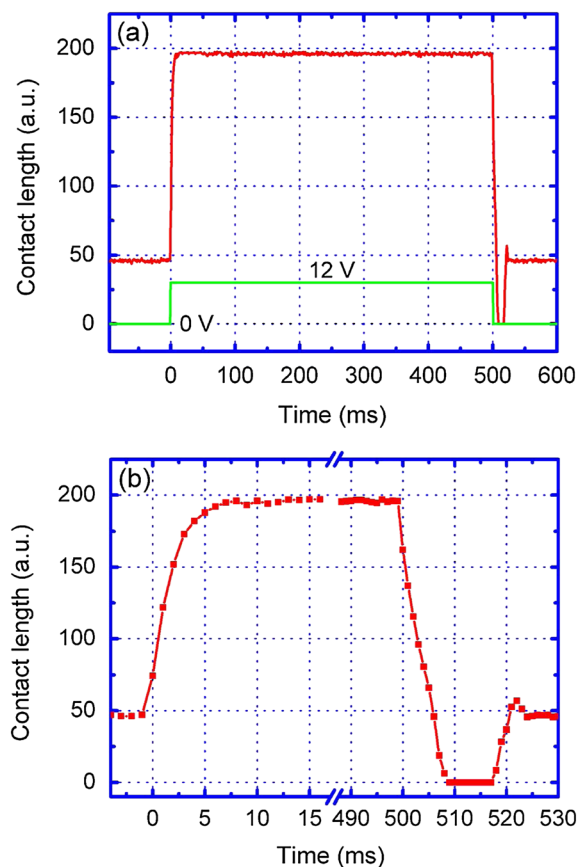


FIGURE 6 — (a) Change in surface contact length of 2 μL (KCl 0.05 M) water droplet in silicone oil under switching of 500 ms, 12 V voltage step and (b) magnified view of the wetting and dewetting switching process.

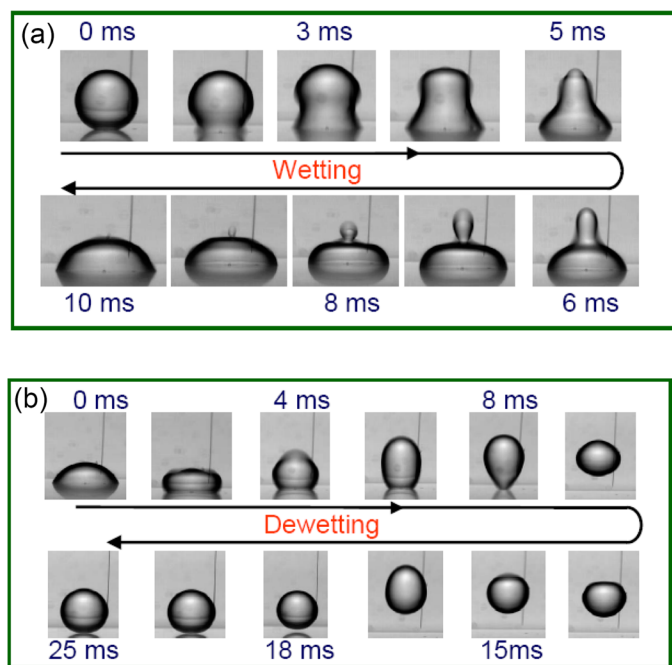


FIGURE 7 — Change in 2 μL (KCl 0.05 M) water droplet shape in silicone oil while switching under a 500 ms voltage step during (a) wetting and (b) dewetting.

and dewetting (Fig. 7b) movement at 1 ms intervals during the 12 V voltage switching process. When the voltage changed from 0 to 12 V (turn-on), the devices showed a wetting (switch-on) time of 7 ms. Changing the voltage from 12 to 0 V (turn-off) results in dewetting (switch-off) times of 8 ms. This result is superior to that of conventional microscope glass slide substrate device¹⁶ which is not surprising given that the Ra of the ultra-thin glass is 0.38 nm, compared with ~ 2 nm for conventional glass slides. In general, the electrolyte concentration in aqueous solution, the addition of surfactant to the aqueous solution, and viscosity of the oil will affect the switching speed.¹⁸ In this work, the wetting and dewetting times of different materials were measured and are summarized in Table 1. The CA changes when the voltage applied are also included for comparison. The 0.05 M KCl water droplet showed nearly the same wetting time of ~ 10 ms for both air and dodecane ambients, but the dewetting time is faster in air. This is due to the fact that the interface tension between the water droplet and air (68.48 dyn/cm) is larger than that between water and dodecane (31.12 dyn/cm). The dewetting and wetting times are improved to 8 and 7 ms, respectively, when the ambient is changed from dodecane (surface tension of 25 mN/m) to silicone oil mixture (16 mN/m), which results in the best performance combination. It is attributed to the penetration of silicone oil into nanopores of the amorphous fluoropolymer layer.²⁴ These switch-on and switch-off times are very promising for video-rate display applications. Adding a surfactant (sodium dodecyl sulfate) at 0.01 and 0.1 wt% in the DI water results in dewetting time increase to 11 and 17 ms, respectively, as the interface tension of the DI water droplet decreased. The wetting times were not improved by the addition of the surfactant because this process is controlled by the applied voltage rather than surface tension. CA change for EW in air is limited by initial CA of DI water on CYTOP surface, which is $115 \sim 120^\circ$. This value is close to the theoretical limit value of the CA of water droplet on any kind of smooth superhydrophobic surface. In most of other cases, the value of ΔCA is between $\sim 40\text{--}50^\circ$. Only by adding a fairly high concentration of surfactant (~ 0.1 wt %) can one increase the ΔCA to $\sim 80^\circ$, with the penalty of much increased dewetting time.

To demonstrate the EW operation on a curved glass surface, Fig. 8a shows a photograph of three water droplets placed on the 100 μm glass substrate prepared for EW experiments being mechanically held in curved position ($\sim 3\text{-cm}$ radius of curvature). The droplets contain water-soluble dyes for visualization purposes. The left (red) and right (green)

TABLE 1 — Wetting and dewetting times for different electrowetting liquids.

Working liquids*	Wetting time (ms)	Dewetting (ms)	ΔCA (deg.)	γ dyn/cm
KCl (0.05 M)/air	10	8	15	68.48
KCl (0.05 M)/dodecane oil	11	20	45	31.12
KCl (0.05 M)/silicone oil	7	8	52	33.75
SDS (0.01 wt%)/silicone oil	7	11	42	31.14
SDS (0.1 wt%)/silicone oil	8	17	78	10.11

KCl and sodium dodecyl sulfate solution in water

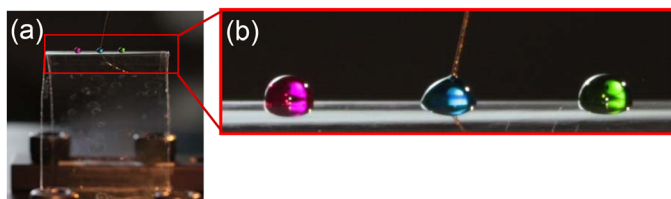


FIGURE 8 — Ultra-thin lightweight glass used for electrowetting on flexible substrate (a) photograph of glass substrate prepared for electrowetting (EW) experiments being held in curved position and (b) close-up photograph of water droplets on EW glass substrate; middle droplet is biased through wire electrode and shows EW action (reduced contact angle).

droplets show the typical high CA on the CYTOP surface. A gold wire is inserted into the middle (blue) droplet, through which the external bias is applied. The EW effect results in the observable change in the CA. Figure 8b shows a close-up photograph of the three water droplets on the curved glass substrate, which allows easy observation of the shape of the blue droplet with applied bias. The substrate can be bent to a radius of ~ 3 cm, during which the EW operation is still maintained. Prototypes of EW arrays with the 100- μm Willow Glass substrate (45×21 array and $300 \times 900 \mu\text{m}^2$ pixel) have been fabricated and a video of operation can be found in the supplementary materials section.

4 Summary and conclusions

We have successfully demonstrated the feasibility of using ultra-thin glass in EW display applications. Although the current EW devices need further improvement, the results clearly indicate the potential of using 100- μm thin glass instead of thicker glass or polymer substrates. The EW devices on ultra-thin glass showed large CA modulation ($\sim 80^\circ$) and very low hysteresis, which is more than sufficient for many EW applications. The fast switching speed obtained (sub-10 ms wetting and dewetting times) is very promising for video display applications. The advantages of using ultra-thin glass for EW (and other) displays include not only a significant reduction in the weight and thickness of the display but also compatibility with R2R process in the future to obtain high volume manufacturing options.

The authors gratefully acknowledge the support of Corning Inc. and useful technical discussions with Dr. Sean Garner.

Supporting Information

Supporting information may be found in the online version of this article.

References

- 1 J. S. Park *et al.*, "Flexible full color organic light-emitting diode display on polyimide plastic substrate driven by amorphous indium gallium zinc oxide thin-film transistors," *Appl. Phys. Lett.* **95**, 013503 (2009).
- 2 J. Heikenfeld, "Lite, brite displays," *IEEE Spectrum* **47**, 28–56 (2010).
- 3 A. J. Steckl, "Circuits on cellulose," *IEEE Spectrum* **50**, 48–61 (2013).
- 4 E. Huitema, "The future of displays is foldable," *Information Display* **28**, 6–10 (2012).
- 5 P. Semenza, "Display glass: bigger, thinner, and stronger," *Information Display* **28**, 6–9 (2012).
- 6 J. A. Rogers *et al.*, "Paper-like electronic displays: large-area rubber-stamped plastic sheets of electronics and microencapsulated electrophoretic inks," *Proc. Natl. Acad. Sci.* **98**, 4835–4840 (2001).
- 7 G. H. Gelinck *et al.*, "Flexible active-matrix displays and shift registers based on solution-processed organic transistors," *Nature Mater.* **3**, 106–110 (2004).
- 8 V. Subramanian *et al.*, "Progress toward development of all-printed RFID tags: materials, processes, and devices," *Proc. IEEE* **93**, 1330 (2005).
- 9 S. Park, and S. Jayaraman, "Smart textiles: wearable electronic systems," *MRS. Bull.* **28**, 585–591 (2003).
- 10 M. Hamedi *et al.*, "Towards woven logic from organic electronic fibres," *Nature Mater.* **6**, 357–362 (2007).
- 11 J. Kim *et al.*, "Reflective and transreflective liquid crystal displays for low-power mobile applications," *Proc. SPIE* **5936**, 593603 (2005).
- 12 F. Mugele, and J. C. Baret, "Electrowetting: from basics to applications," *J. Phys. Condens. Matter* **17**, R705–R774 (2005).
- 13 C. Quilliet, and B. Berge, "Electrowetting: a recent outbreak," *Curr. Opin. Colloid Interface Sci.* **6**, 34–39, 2001.
- 14 D. Y. Kim, and A. J. Steckl, "Complementary electrowetting devices on plasma-treated fluoropolymer surfaces," *Langmuir* **26**, 9474–9483 (2010).
- 15 R. A. Hayes, and B. J. Feenstra, "Video-speed electronic paper based on electrowetting," *Nature* **425**, 383–385 (2003).
- 16 H. You, and A. J. Steckl, "Three-color electrowetting display device for electronic paper," *Appl. Phys. Lett.* **97**, 023514 (2010).
- 17 D. Y. Kim, and A. J. Steckl, "Electrowetting on paper for electronic paper display," *ACS Appl. Mater. Interfaces* **2**, 3318–3323 (2010).
- 18 H. You, and A. J. Steckl, "Electrowetting on flexible substrates," *J. Adhes. Sci. Technol.* **26**, 1931–1939 (2012).
- 19 A. J. Steckl *et al.*, "Electrowetting: a flexible electronic-paper technology," *SPIE Newsroom*, DOI: 10.1117/2.1201101.003443, 2011.
- 20 J. S. Lewis, and M. S. Weaver, "Thin-film permeation-barrier technology for flexible organic light-emitting devices," *IEEE J. Sel. Top. Quantum Electron.* **10**, 45–57 (2004).
- 21 P. Lo *et al.*, "Flexible glass substrates for organic TFT active matrix electrophoretic displays," *SID Symposium Digest* **42**, 387–388 (2011).
- 22 S. M. Garner *et al.*, "Electrophoretic displays fabricated on ultra-slim flexible glass substrates," *J. Display Technol.* **8**, 590–595 (2012).
- 23 Corning Willow Glass Fact Sheet; www.corning.com.
- 24 H. J. Verheijen, and M. W. J. Prins, "Reversible electrowetting and trapping of charge: model and experiments," *Langmuir* **15**, 6616–6620 (1999).



Han You received his PhD degree in Polymer Chemistry and Physics from Changchun Institution of Applied Chemistry, Chinese Academy of Science (China). After receiving his PhD, he moved to Nanoelectronics Laboratory in University of Cincinnati as a postdoctoral researcher fellow. His research interest is focused on organic electronic device and electrowetting devices.



Dr. Andrew J. Steckl is an Ohio Eminent Scholar and Carl Gieringer Professor of Solid State Electronics at the University of Cincinnati, where he directs the Nanoelectronics Laboratory. He has been a faculty member at Cincinnati since 1988. Previously, he was on the faculty at Rensselaer Polytechnic Institute, where he founded the Center for Integrated Electronics. Dr. Steckl obtained his BS from Princeton and his PhD from the University of Rochester. Dr. Steckl is a fellow of Institute of Electrical and Electronics Engineers and American Association for the Advancement of Science. At Cincinnati, he received numerous awards, including the Rieveschl Award for Distinguished Scientific Research, Distinguished Engineering Research Award, and Graduate Faculty Fellow. In 2013, he was named Distinguished Research Professor. Dr. Steckl's current research areas of interest include (organic and inorganic) light emitting materials and devices and electrofluidics (electrowetting and electrospinning). Together with his students, he has published over 400 articles and obtained 14 patents, with a current citation h-index of 46.